

Final Technical Report

FA9550-05-1-0139

'Plastic' Optoelectronics: Injection Lasers Fabricated from Soluble
Semiconducting Polymers and Bulk Heterojunction Solar Cells Fabricated
from Soluble Semiconducting Polymers

Dr. Charles Lee, Program Director
801 N. Randolph Street, Room 732
Arlington, VA 22203

Institute for Polymers and Organic Solids
University of California, Santa Barbara
Santa Barbara, CA 93106

Principal Investigators:

Professor Alan J. Heeger

Soc. Sec. # 508-34-6588

Phone: (805) 893-3184

Mobile phone: (805) 570-9053

FAX: (805) 893-4755

ajhe@physics.ucsb.edu

Physics Department and Materials Department (joint appointment)

Professor Guillermo Bazan

Soc. Sec. # 032-665-642

Phone: (805) 893-5538

FAX: (805) 893-4755

bazan@chem.ucsb.edu

Chemistry Department and Materials Department (joint appointment)

20080516052



DEFENSE TECHNICAL INFORMATION CENTER

Information for the Defense Community

DTIC[®] has determined on

Month	Day	Year
06	11	2008

 that this Technical Document has the Distribution Statement checked below. The current distribution for this document can be found in the DTIC[®] Technical Report Database.

- DISTRIBUTION STATEMENT A.** Approved for public release; distribution is unlimited.
- © COPYRIGHTED.** U.S. Government or Federal Rights License. All other rights and uses except those permitted by copyright law are reserved by the copyright owner.
- DISTRIBUTION STATEMENT B.** Distribution authorized to U.S. Government agencies only. Other requests for this document shall be referred to controlling office.
- DISTRIBUTION STATEMENT C.** Distribution authorized to U.S. Government Agencies and their contractors. Other requests for this document shall be referred to controlling office.
- DISTRIBUTION STATEMENT D.** Distribution authorized to the Department of Defense and U.S. DoD contractors only. Other requests shall be referred to controlling office.
- DISTRIBUTION STATEMENT E.** Distribution authorized to DoD Components only. Other requests shall be referred to controlling office.
- DISTRIBUTION STATEMENT F.** Further dissemination only as directed by controlling office or higher DoD authority.
- Distribution Statement F is also used when a document does not contain a distribution statement and no distribution statement can be determined.*
- DISTRIBUTION STATEMENT X.** Distribution authorized to U.S. Government Agencies and private individuals or enterprises eligible to obtain export-controlled technical data in accordance with DoDD 5230.25.

REPORT DOCUMENTATION PAGE

Form Approved
OMB No. 0704-0188

The public reporting burden for this collection of information is estimated to average 1 hour per response, including the time for reviewing instructions, searching existing data sources, gathering and maintaining the data needed, and completing and reviewing the collection of information. Send comments regarding this burden estimate or any other aspect of this collection of information, including suggestions for reducing the burden, to the Department of Defense, Executive Service Directorate (0704-0188). Respondents should be aware that notwithstanding any other provision of law, no person shall be subject to any penalty for failing to comply with a collection of information if it does not display a currently valid OMB control number.

PLEASE DO NOT RETURN YOUR FORM TO THE ABOVE ORGANIZATION.

1. REPORT DATE (DD-MM-YYYY) 17-04-2008	2. REPORT TYPE Final Performance	3. DATES COVERED (From - To) 2/15/05-12/31/07
--	--	---

4. TITLE AND SUBTITLE 'Plastic' Optoelectronics: Injection Lasers Fabricated from Soluble Semiconducting Polymers and Bulk Heterojunction Solar Cells	5a. CONTRACT NUMBER
	5b. GRANT NUMBER FA9550-05-1-0139
	5c. PROGRAM ELEMENT NUMBER

6. AUTHOR(S) Dr. Alan J. Heeger Dr. Guillermo C. Bazan	5d. PROJECT NUMBER
	5e. TASK NUMBER
	5f. WORK UNIT NUMBER

7. PERFORMING ORGANIZATION NAME(S) AND ADDRESS(ES) The Regents of the University of California Center for Polymers and Organic Solids, University of California Santa Barbara, CA 93106	8. PERFORMING ORGANIZATION REPORT NUMBER
---	---

9. SPONSORING/MONITORING AGENCY NAME(S) AND ADDRESS(ES) Air Force Office of Scientific Research 875 N Randolph St Arlington VA 22203 Dr Charles Lee/NA	10. SPONSOR/MONITOR'S ACRONYM(S) AFOSR
	11. SPONSOR/MONITOR'S REPORT NUMBER(S)

12. DISTRIBUTION/AVAILABILITY STATEMENT Available for distribution	AFRL-SR-AR-TR-08-0233
--	-----------------------

13. SUPPLEMENTARY NOTES

14. ABSTRACT
We summarize progress on bulk heterojunction (BHJ) "plastic" solar cells: BHJ solar cells are based on phase-separated blends of polymer semiconductors and fullerene derivatives. Because of self-assembly on the nanometer length-scale, excitons formed after absorption of solar irradiation diffuse to a heterojunction prior to recombination and are dissociated at the polymer/fullerene interface. Ultrafast charge transfer from semiconducting polymers to fullerenes guarantees that the quantum efficiency for charge transfer (CT) at the interface approaches unity, with electrons on the fullerene network and holes on the polymer network. Electrons migrate toward the lower work function metal and holes migrate toward the higher work function metal. Carrier recombination prior to reaching the electrodes and low mobility limit both the device fill factor (FF) and the overall photon harvesting by reducing the optimum active layer thickness. The carrier lifetime is largely controlled by the phase morphology between the donor and acceptor materials.
We also summarize the results obtained to demonstrate the realization of the Light emitting Field effect Transistors.

15. SUBJECT TERMS
polymer solar cells, light-emitting field effect transistors

16. SECURITY CLASSIFICATION OF:			17. LIMITATION OF ABSTRACT UU	18. NUMBER OF PAGES 12	19a. NAME OF RESPONSIBLE PERSON Dr. Alan J. Heeger
a. REPORT None	b. ABSTRACT None	c. THIS PAGE none			19b. TELEPHONE NUMBER (Include area code) 805-893-3184

I. Light weight and Low Cost Polymer Based BHJ Solar Cells: Recent Progress at UCSB

a. Titanium-oxide Films as Multifunctional Components in BHJ “Plastic” Solar Cells

Bulk heterojunction “plastic” solar cells are based on phase-separated blends of polymer semiconductors and fullerene derivatives. Because of self-assembly on the nanometer length-scale, excitons formed after absorption of solar irradiation diffuse to a heterojunction prior to recombination and are dissociated at the polymer/fullerene interface. Ultrafast charge transfer from semiconducting polymers to fullerenes guarantees that the quantum efficiency for charge transfer (CT) at the interface approaches unity, with electrons on the fullerene network and holes on the polymer network. After breaking the symmetry by using different metals for the two electrodes, electrons migrate toward the lower work function metal and holes migrate toward the higher work function metal. Carrier recombination prior to reaching the electrodes and low mobility limit both the device fill factor (FF) and the overall photon harvesting by reducing the optimum active layer thickness. The carrier lifetime is largely controlled by the phase morphology between the donor and acceptor materials.

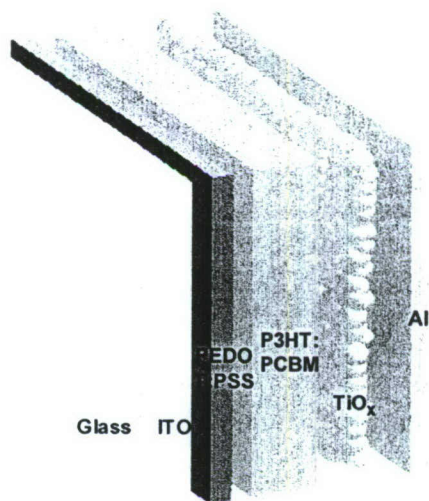
In the following paragraphs, we summarize the recent progress enabled by including one or more layers of titanium sub-oxide, TiO_x , into the architecture of bulk heterojunction solar cells. The use of TiO_x provides several important opportunities; specifically, the TiO_x layers enable higher performance from single cells, longer lifetime as a result of reduced sensitivity to oxygen and water vapor, and the fabrication of bulk heterojunction cells in the “Tandem Cell” architecture, a multilayer structure that is equivalent to two photovoltaic cells in series.

b. Sol-gel Processed Titanium Oxide as an Optical Spacer in Polymer Solar Cells

In the standard BHJ solar cell structure, the intensity of the light is zero at the metallic (e.g Al) back electrode because of optical interference between the incident light (from the ITO side) and the back-reflected light. Thus, a relatively large fraction of the active charge separating layer is in a dead-zone in which the photogeneration of carriers is significantly reduced. This optical interference effect is especially important for thin film structures where layer thicknesses are comparable to the absorption depth and the wavelength of the incident light, as is the case for photovoltaic cells fabricated from semiconducting polymers. In order to overcome these problems, one might simply increase the thickness of the active layer to absorb more light. Because of the low mobility of the charge carriers in the polymer/ C_{60} composites, however, the increased internal resistance of thicker films will inevitably lead to a reduced fill factor (FF).

An alternative approach is to change the device architecture with the goal of spatially redistributing the light intensity inside the device by introducing an optical spacer between the active layer and the Al electrode. The optical spacer layer must be a good acceptor and an electron transport material with a conduction band edge lower in energy than that of the lowest unoccupied molecular orbital (LUMO) of C_{60} , the conduction band edge must be above (or close to) the Fermi energy of the collecting metal electrode, and the material must be transparent to light with wavelengths within the solar spectrum.

Titanium dioxide (TiO_2) is a promising candidate as an electron acceptor and transport material. Typically, however, crystalline TiO_2 is used either in the anatase phase or the rutile phase, both of which require treatment at temperatures ($T > 450^\circ\text{C}$) that are inconsistent with the fabrication of “plastic” solar cells; the polymer/ C_{60} composite cannot survive such high temperatures. To solve this problem, we have used sol-gel chemistry to create amorphous TiO_x films with properties that meet all the requirements [J. Y. Kim, S. H. Kim, H.-H Lee, K. Lee, W. Ma, X. Gong, A. J. Heeger, *Adv. Mater.* **2006**, *18*, 572].

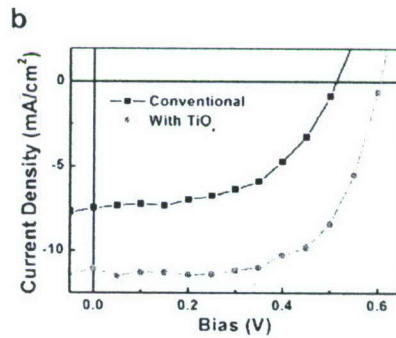
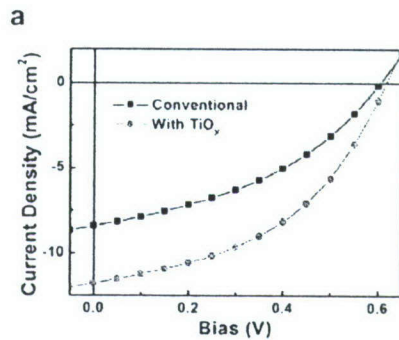


Utilizing the TiO_x layer as the optical spacer, donor/acceptor composite photovoltaic cells were fabricated using the phase separated BHJ material comprising poly(3-hexylthiophene) (P3HT) as the electron donor and the fullerene derivative, [6,6]-phenyl- C_{61} butyric acid methyl ester (PCBM) as the acceptor. The device structure is shown in the Figure above.

For the device with the TiO_x optical spacer, the incident photon to current collection efficiency spectrum (IPCE) data demonstrate substantial enhancement over the entire excitation spectral range; the maximum reaches almost 90% at 500 nm, corresponding to a 50% increase in IPCE. Since surface reflection from the glass is approximately 10%, the optical spacer enhances the efficiency to $> 90\%$ for light incident with wavelengths in the range 450 – 550 nm. This enhancement is the result of increased absorption in the bulk heterojunction layer as a result of the TiO_x optical spacer; the increased photo-generation of charge carriers results from the spatial redistribution of the light intensity.

As shown in the Figure below, the enhancement in the device efficiency that results from the optical spacer can be directly observed in the current density vs voltage (I-V) characteristics.

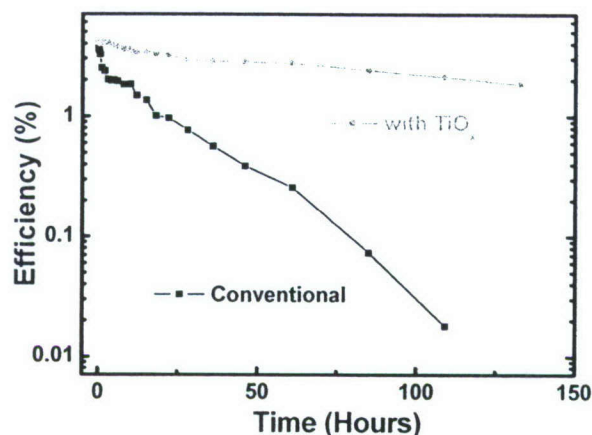
- For Green light (532 nm), the efficiency improves from $\eta = 8.1\% \rightarrow 12.6\%$.
- Under AM1.5 (solar spectrum), the efficiency improves from $\eta = 2.3\% \rightarrow 5.0\%$.



c. Air-stable Bulk Heterojunction Polymer Solar Cells

The degradation of devices fabricated from semiconducting polymers (e.g. polymer LEDs and bulk heterojunction solar cells) can be eliminated, or at least reduced to acceptable levels, by sealing the components inside an impermeable package using glass and/or metal. To achieve the goal of printed “plastic” electronics, either the development of improved barrier materials for packaging or the development of devices with reduced sensitivity (or both) are required. Thus, the creation of new methods for enhancing device lifetime is an important goal that must be accomplished without interfering with the principal ‘flexible device’ concepts; simple fabrication by solution processing, flexibility, and thin form factor.

Using the solution-based sol-gel process, described above as a collector and optical spacer for bulk heterojunction solar cells, the device lifetime, unpackaged and in air, is significantly enhanced [K. Lee, J.Y Kim,, S.H. Park, S.H. Kim, S. Cho and A.J. Heeger, *Adv. Mater.*19, 2445(2007)] As shown in the Figure below, the lifetime is enhanced by a factor of approximately 100!



The achievement of 'air-stable' polymer devices implies that the promise of high performance 'flexible' and 'printable' devices can be realized with significantly enhanced device lifetimes. *Since the TiO_x layer is generated by a sol-gel process, all fabrication steps are carried out by processing the component materials from solution; i.e. consistent with printing and coating technologies. The TiO_x layer reduces the sensitivity to oxygen and water vapor to a point where simple barrier materials might be sufficient to enable the lifetimes required for printed, flexible, plastic electronics.*

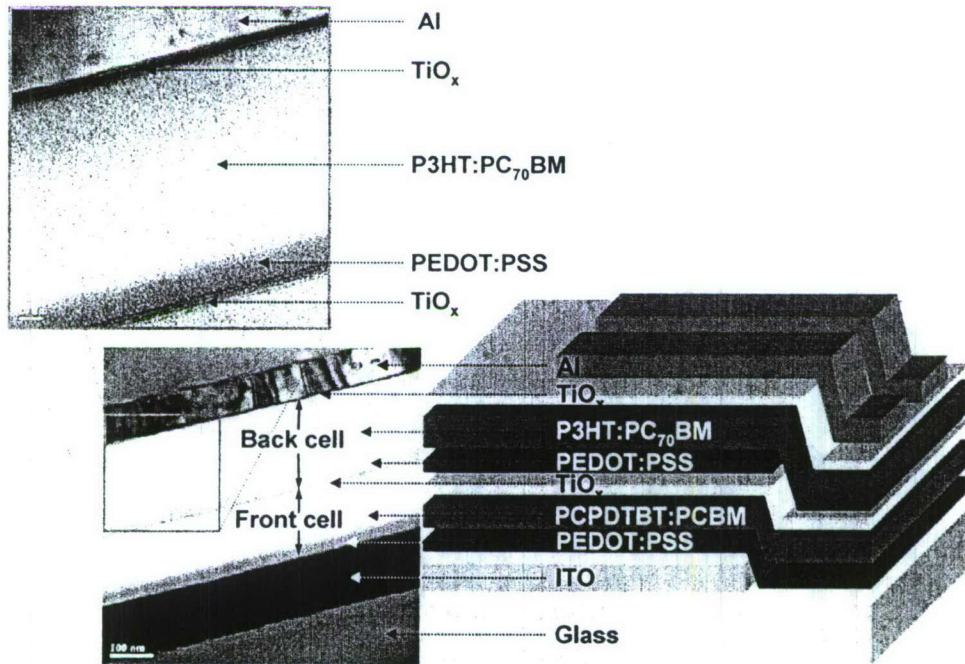
d. Efficient Polymer Solar Cells in the Tandem Architecture

The 'Tandem Cell' architecture, a multilayer structure that is equivalent to two photovoltaic cells in series, offers a number of advantages. Because the two cells are in series, the open circuit voltage (V_{oc}) is increased to the sum of the V_{oc} 's of the individual cells. The use of two semiconductors with different band gaps enables absorption over a broad range of photon energies within the solar emission spectrum; the two cells typically utilize a wide band gap semiconductor for the first cell and a smaller bandgap semiconductor for the second cell. Since the electron-hole pairs generated by photons with energies greater than the energy gap rapidly relax to the respective band edges, the power conversion efficiency of the two cells in series is inherently better than that of a single cell made from the smaller band gap material. Moreover, because of the low mobility of the charge carriers in the polymer-fullerene composites, an increase in the thickness of the active layer increases the internal resistance of the device, which reduces both the V_{oc} and fill factor (FF). Thus, the tandem cell architecture can have a higher optical density over a wider fraction of the solar emission spectrum than a single cell without increasing the internal resistance. The tandem cell architecture can therefore improve the light harvesting in polymer based photovoltaic cells.

Polymer tandem cells have recently been successfully demonstrated, with each layer processed from solution, by using the solution-processed TiO_x as the separation layer between the front cell and back cell. The performance of these initial tandem solar cells is summarized as follows: $J_{sc} = 7.8 \text{ mA/cm}^2$, $V_{oc} = 1.24 \text{ V}$, $FF = 0.67$ and $\eta_e = 6.5\%$ [J.Y.

Kim, K. Lee, N. E. Coates, D. Moses, T-Q. Nguyen, M. Dante and A. J. Heeger, Science 13, 222 (2007)].

The structure of the multilayer polymer tandem solar cell is shown in the Figure below. The charge separation layer for the front cell is a bulk heterojunction composite of poly[2,6-(4,4-bis-(2-ethylhexyl)-4H-cyclopenta[2,1-b;3,4-b']dithiophene)-alt-4,7-(2,1,3-benzothiadiazole)], (PCPDTBT) and [6,6]-phenyl-C61butyric acid methyl ester (PCBM). The charge separation layer for the back cell is a bulk heterojunction composite of P3HT and [6,6]-phenyl-C71 butyric acid methyl ester (PC₇₀BM). The two polymer-fullerene layers are separated by a transparent TiO_x layer and a highly conductive hole transport layer, PEDOT:PSS (Baytron PH500). Electrons from the first cell combine with holes from the second cell at the TiO_x – PEDOT:PSS interface.



Cross-sectional images of the polymer tandem solar cells were taken with high resolution transmission electron microscopy (TEM); the individual layers are clearly seen. Perhaps more important, the various interfaces are remarkably sharp; there is no inter-layer mixing.

Optimization of the Tandem Cell device sketched above, more than 20 tandem cells were fabricated with efficiencies above 6.2%; typical performance parameters were as follows; $J_{sc} = 7.8 \text{ mA/cm}^2$, $V_{oc} = 1.24 \text{ V}$, $FF = 0.67$ and $\eta_e = 6.5\%$.

In summary, the sol-gel processed TiO_x layer serves multiple functions:

1. Deposited between the charge separation layer (BHJ phase separated mixture) and the Al cathode, the TiO_x functions as an optical spacer that redistributes the light intensity to optimize the efficiency.

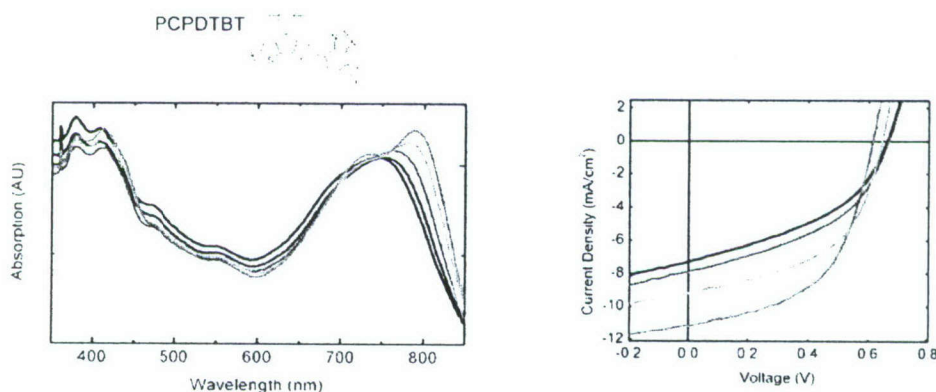
2. By introducing a TiO_x layer between the charge separating layer and the Al cathode, excellent air stability has been demonstrated. The TiO_x layer improves the lifetime of unpackaged devices by nearly two orders of magnitude.
3. The TiO_x functions as an electron transport layer and a hole blocking layer and thereby enhances carrier collection at the electrodes.

The TiO_x layer enables the fabrication of tandem cells. The transparent TiO_x layer is used to separate and connect the front cell and the back cell. The TiO_x layer serves as an electron transport and collecting layer for the first cell and as a stable foundation that enables the fabrication of the second cell to complete the tandem cell architecture.

e. Processing additives as a route to morphology control in BHJ Solar Cells

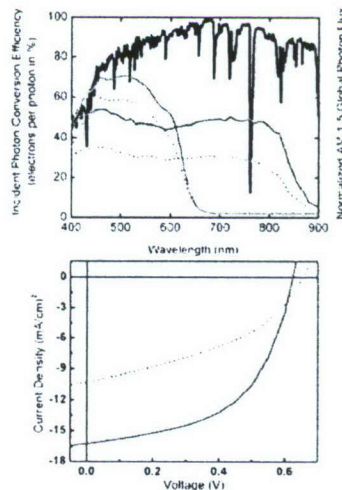
Attempts to control the donor/acceptor morphology in BHJ materials as required for achieving high power conversion efficiency have met with limited success. By incorporating a few volume percent of alkanedithiols in the solution used to spin cast films comprising a low bandgap polymer and a fullerene derivative, the power conversion efficiency of photovoltaic cells (AM 1.5G conditions) is increased from 2.8% to 5.5% through altering the bulk heterojunction morphology [Peet, J.; Kim, J. Y.; Coates, N. E.; Ma, W. L.; Moses, D.; Heeger, A. J.; Bazan, G. C. *Nature Mater.* 6, 497-500 (2007).].

The Figure below (left) shows the shift in the film absorption caused by adding different alkanedithiols to the PCPDTBT: C_{71} -PCBM solution in chlorobenzene (CB) prior to spin casting. One observes the largest change with the addition of 2.4 mg/mL of 1,8-octanedithiol into the chlorobenzene solution; the film absorption peak red-shifts 41 nm to 800 nm. Such a shift to lower energies and the emergence of structure on the absorption peak associated with the π - π^* transition when films are processed with alkanedithiols indicates that the PCPDTBT chains interact more strongly and that there is improved local structural order compared with films processed from pure CB. The Figure below (right) shows clearly the increase in I_{sc} and the increase in FF that result from the use of the processing additive.



As demonstrated in the Figure below, by processing the BHJ film using 1,8-octanedithiol as a processing additive, the solar conversion efficiency can be increased by a factor of two. The results shown in the lower panel indicate a power conversion efficiency of 5.5 %, an increase by a factor of two over that obtained from the same

polymer but without the use of the 1,8-octanedithiol; this represents the highest efficiency yet reported for a single cell (our Tandem Cell architecture has yielded 6.5% --- see above). The approach described here provides an operationally simple and versatile tool available for the tailoring of the heterojunction solar cell morphology in systems where thermal annealing is not effective. Note that this new approach works even on a system in which polymer crystallinity is not observed. Based on calculations by Brabec et. al. on photovoltaic cells fabricated from PCPDTBT:C₇₁-PCBM, further optimization of morphology and equalization of bipolar transport could lead to power conversion efficiencies as high as 7%. This expectation is fully consistent with the ICPE data shown above; there is a clear opportunity to increase the IPCE.



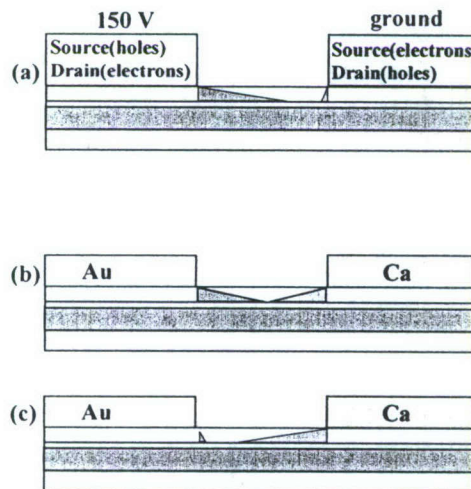
Top: IPCE spectra of polymer bulk heterojunction solar cells composed of P3HT:C₆₁-PCBM before (dotted red) and after (solid red) annealing, and PCPDTBT:C₇₁-PCBM with (solid green) and without (dotted green) the use of 1,8-octanedithiol. The AM 1.5 global reference spectrum is shown for reference (black).

Bottom: Current voltage characteristics of the same PCPDTBT devices used for the IPCE measurements, processed with (solid) and without (dotted line) 1,8-octanedithiol under 100 mW/cm² AM 1.5G illumination; $I_{sc} = 16.2 \text{ mA/cm}^2$, $FF = 0.55$, and $V_{oc} = 0.62 \text{ V}$.

II. Light Emitting Field Effect Transistors (LEFETs) as the route to “plastic” injection lasers

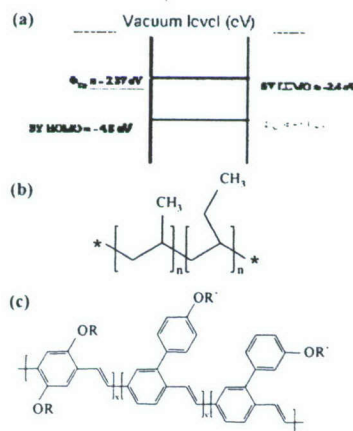
The architecture of the LEFET is shown in the Figure below [J. S. Swensen, C. Soci, and A. J. Heeger, *Applied Physics Letters* 87, 253511 (2005); J. Zaumseil, R. H. Friend, and H. Sirringhaus, *Nature Materials* 5, 69-74 (2006). J.S. Swensen, D. Gargas, J. Yuen, S. Buratto and Alan J. Heeger, *J. Appl. Phys.* 102, 013103 (2007)]. The structure is similar to that of conventional FETs, with a dielectric layer separating the gate from the semiconducting material. The high work function electrode serves as the source for holes into the π -band and the drain for electrons from the π^* -band, $S_h(D_e)$; the low work function electrode serves as the source for electrons into the π^* -band and the drain for holes from the π -band, $S_e(D_h)$. Under conditions of balanced electron and hole currents,

the LEFET can be viewed as a gate-induced p-n junction (see Fig (b) below); light emission is expected and observed only in a narrow zone where the electron accumulation layer and the hole accumulation layer overlap.

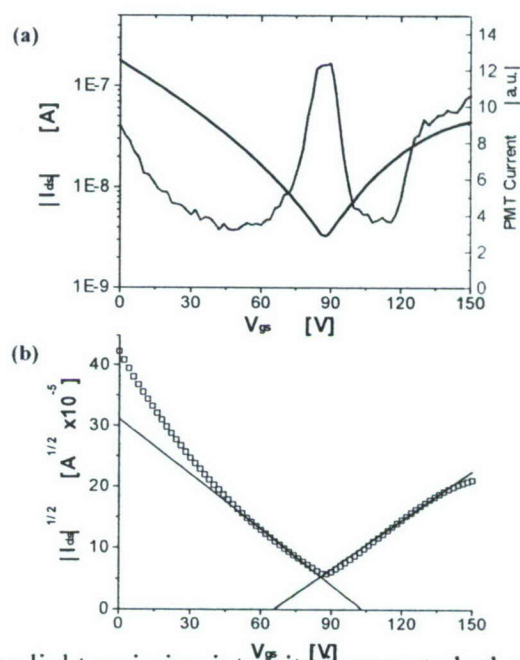


As shown in (a) and (c), at the gate voltage extremes ($V_G = 0$ or $V_G = 150$ V), the electron (hole) density extends across the $16 \mu\text{m}$ channel such that the electron (hole) accumulation layer functions as the cathode (anode) for an LED, with opposite carrier injection by tunneling; i.e. the carrier densities are sufficiently high that the accumulation layer functions as a low resistance contact, implying near metallic transport.

The Figure below shows the energy level diagram of the luminescent semiconducting polymer, "SuperYellow" used in the LEFET. The Fermi energies of Ca and Au are also shown. The molecular structures of the passivating polypropylene-co-1-butene (PPcB) and of Super Yellow (SY) are also shown in the Figure.



The transfer (transconductance) data are shown in the Figure below; channel current vs. gate voltage and emitted light intensity vs. gate voltage for an LEFET made with Au and Ca as the two electrode materials. The black curve represents the total current between the Au (the source for holes into the π -band and the drain for electrons from the π^* -band) and Ca (the source for electrons into the π^* -band and the drain for holes from the π -band) electrodes as a function of the voltage applied at the gate electrode. The blue curve shows the light emission intensity. Note the near-symmetry of both the channel current vs. gate voltage and the emitted light intensity vs. gate voltage (significantly better than observed with Ag as the high work function metal).



Maximum light emission intensity is expected when hole and electron currents are balanced, i.e. when each injected electron (hole) can radiatively recombine with a hole (electron). Because of the difference in hole and electron mobilities ($\mu_h > \mu_e$), this maximum occurs at approximately 90 V, rather than at 75 V (the mid-point in the range of the scan of the gate voltage).

Note that at the voltage extremes, the emission intensity again increases. For example, at the beginning of the scan when the gate voltage equals 0 V, the device was emitting light. By imaging the channel with a microscope at 40x magnification, the emission zone was observed to be along the edge of the channel next to the calcium $S_e(D_h)$ electrode. We interpret this light emitted when $V_g = 0$ V as arising from more conventional emission from a polymer light-emitting diode (LED). A similar emission process has been discussed for hole only organic LEFETs, and, in fact, it is likely the mechanism for light emission in all unipolar organic "LEFETs". As sketched in Fig. 1a, when $V_g \rightarrow 0$, the hole density extends across the 16 μm channel length such that the hole

accumulation layer functions as the anode for an LED with electron injection by tunneling from the Ca electrode. Similarly, as sketched in Fig. 1c, when $V_g \rightarrow -150$ V with respect to the Ca electrode, the electron density extends across the 16 μm channel length such that the electron accumulation layer functions as the cathode for an LED with hole injection by tunneling from the Au electrode. In these two limits, the carrier densities (electrons in the π^* - band or holes in the π - band) are sufficiently high that the accumulation layer functions as a low resistance contact, implying near metallic transport.

In the saturation regime (where the source-drain voltage is larger than the gate voltage), the threshold voltages, V_{th} , can be determined from Eqn 1.

$$I_d = \mu C_i \frac{W}{2L} (V_g - V_{th})^2$$

Thus, the threshold voltages for the onset of electron transport, $V_{th}(el)$, and for the onset of hole transport, $V_{th}(h)$, are defined by plotting $|I_{ds}|^{1/2}$ vs. V_g , where I_{ds} is the total current between the Au and Ca electrodes, and extrapolating the electron dominated current and the hole dominated curves, respectively. The linear extrapolations yield the voltages for the turn-on of the hole current (103 Volts between the gate and the grounded Ca electrode) and for the turn-on of the electron current (65 Volts between the gate and the grounded Ca electrode). Thus, $|V_{th}(el)| \approx 65$ V and $|V_{th}(h)| = 150$ V - 103 V ≈ 47 V indicative of significant disorder with traps at the semiconductor-dielectric interface.⁶ Only for $V_g = 65$ V $< V_G < 103$ V, the device operates in the ambipolar regime with electrons in the π^* -band and holes in the π -band. The electron and hole mobilities were obtained from the slopes of the extrapolated lines: $\mu_h = 2.1 \times 10^{-5}$ cm²/V/sec and $\mu_e = 1.6 \times 10^{-5}$ cm²/V/sec.

In the LEFET under ambipolar conditions, light emission is expected only in a narrow zone where the electron accumulation layer and the hole accumulation layer overlap. Therefore, in the ambipolar regime, the location of the emission zone is controlled by the gate bias and moves across the channel. Smith and Ruden [D. L. Smith and P. P. Ruden, Applied Physics Letters 89, 233519 (2006)] calculated the gate-to-channel potential and the associated carrier densities (electrons and holes) as a function of distance within the channel, assuming (initially) an infinite recombination rate. Their calculations show that the gate to channel potential goes to zero, where the hole and electron accumulation regions begin to overlap. This location, which moves as the voltage is scanned across the ambipolar region, defines the center of the light emission zone. In the limit of infinite recombination rate, the recombination zone (and thus the emission zone) would be infinitely narrow. In reality, however, the width of the emission zone is determined by the recombination rate; the smaller the recombination rate, the wider the emission zone.

The emission zone has been spatially resolved using confocal microscopy. Analysis of the spatial intensity profile shows that the full width at half maximum of the emission zone is consistently 2 μm as it moves across the channel.

At the voltage extremes, for example when the gate voltage approaches -150 V with respect to the $S_e(D_h)$ electrode (Ca), the electron density extends all the way across the 16 μm channel length such that the electron accumulation layer functions as the cathode for an LED with hole injection by tunneling from the Au electrode. Similarly, when the gate voltage approaches +150 V with respect to the $S_h(D_e)$ electrode (Au), the

electron density extends all the way across the 16 μm channel length such that the hole accumulation layer functions as the anode for an LED with electron injection by tunneling from the Ca electrode. In other words, in these two limits the carrier densities (electrons in the π^* - band or holes in the π - band) are sufficiently high that the accumulation layer functions as a low resistance contact, implying near metallic transport. These very long distances for electron and hole accumulation, respectively, more than 10,000 repeat units on the semiconducting polymer chain and more than 10,000 interchain spacings imply the existence of well-defined π - and π^* - bands with a very low density of deep traps within the band gap. Since "SuperYellow" is relatively highly disordered when spin-cast from solution, we conclude that the well-defined band structure with a relatively low density of deep traps within the energy gap is a robust feature of semiconducting polymers.

The LEFET results summarized in this report indicate that in the ambipolar regime, there is population inversion in the semiconducting polymer, with a high density of electrons in the π^ -band ($>10^{19} \text{ cm}^{-3}$ in the region near the interface between the semiconductor and the gate dielectric) and a high density of holes in the π -band (again $>10^{19} \text{ cm}^{-3}$ in the region near the interface between the semiconductor and the gate dielectric). Thus, the LEFET provides a realistic route toward the fabrication of an injection laser from semiconducting polymers.*

Publications:

1. The Fluorescence Resonance Energy Transfer (FRET) Gate: A Time Resolved-Study, A. Xu, S. Wang, D. Korystov, A. Mikhailovsky, G.C. Bazan, D. Moses, A.J. Heeger, PNAS 102, (N3) 530-535 (2005).
2. Light Emission in the Channel Region of a Polymer Thin-Film Transistor Fabricated with Gold and Aluminum for the Source and Drain Electrodes, J. Swensen, D. Moses, A.J. Heeger, Synth. Met. 153 53-56 (2005).
3. Thermally Stable, Efficient Polymer Solar Cells with Nanoscale Control of the Interpenetrating Network Morphology, W. Ma, C. Yang, K. Lee, A.J. Heeger, Adv. Func. Mater. 15 1617-1622 (2005).
5. Light Emission From an Ambipolar Semiconducting Polymer Field Effect Transistor James Swensen, Cesare Soci and Alan J. Heeger, Appl.Phys.Lett. 87, 253511 (2005).
6. Light Emission in the Channel Region of a Polymer Thin-Film Transistor Fabricated with Gold and Aluminum for the Source and Drain Electrodes, J. Swensen, D. Moses, A.J. Heeger, Synth. Met. 153 53-56 (2005).
7. Polymer-Based Light-Emitting Diodes (PLEDs) and Displays Fabricated from Arrays of PLEDs, X. Gong, D. Moses, A.J. Heeger, Organic Light-Emitting Devices: Synthesis, Properties, and Applications, Ed. Klaus Müllen and Ullrich Scherf. Germany: Wiley-VCH, 2006. 151-180.

8. Photoconductivity of a Low-Bandgap Conjugated Polymer. C. Soci, I.W. Hwang, D. Moses, Z. Zhu, D. Waller, R. Gaudiana, C.J. Brabec, A.J. Heeger, Adv. Func. Mater. **17**, (4) 632-636 (2007).
9. Spatial Fourier-Transform Analysis of the Morphology of Bulk Heterojunction Materials Used in "Plastic" Solar Cells, W. Ma, C. Yang, A. J. Heeger, Adv. Mater. **19** (10) 1387-1390 (2007).
10. Ultrafast Spectroscopic Study of Photoinduced Electron Transfer in an Oligo(thienylenevinylene):Fullerene Composite, I.-W. Hwang, Q.-H Xu, C. Soci, A. Jen, D. Moses, A. J. Heeger, Adv. Funct. Mater., **17**, 563, (2007).
11. Light Emission in the Channel Region of a Polymer Thin-Film Transistor Fabricated with Gold and Aluminum for the Source and Drain Electrodes, J. Swensen, D. Moses, A.J. Heeger, Synth. Met. **153** 53-56 (2005).
12. Polymer-Based Light-Emitting Diodes (PLEDs) and Displays Fabricated from Arrays of PLEDs, X. Gong, D. Moses, A.J. Heeger, Organic Light-Emitting Devices: Synthesis, Properties, and Applications, Ed. Klaus Müllen and Ullrich Scherf. Germany: Wiley-VCH, 2006. 151-180.
13. Light emission from an ambipolar semiconducting polymer field effect transistor: Analysis of the device physics, J. S. Swensen, J. Yuen, D. Gargas, S. K. Buratto, A. J. Heeger, J. Appl. Phys. **102**, 013103 (2007).
14. Air-stable polymer electronic devices, Kwanghee Lee, Jin Young Kim, Sung Heum Park, Sun Hee Kim, Shinuk Cho, and Alan J. Heeger, Advanced Materials, **19**, 2445 (2007)
15. Nanostructure of the Interpenetrating Networks in Poly(3-hexylthiophene)/fullerene Bulk Heterojunction Materials: Implications for Charge Transport, Wanli Ma, Ajay Gopinathan and Alan J. Heeger, Advanced Materials, **19**, 3656 (2007).
16. Processing Additives for Improved Efficiency from Bulk Heterojunction Solar Cells, Jae Kwan Lee, Wan Li Ma, Christoph J. Brabec, Jonathan Yuen, Ji Sun Moon, Jin Young Kim, Kwanghee Lee, Guillermo C. Bazan, and Alan J. Heeger, J Amer. Chem. Soc. **130**, 3619 (2008).
17. New Architecture for High-Efficiency Polymer Photovoltaic Cells Using Solution-Based Titanium Oxide as an Optical Spacer, J.Y. Kim, S.H. Kim, H.-H. Lee, K. Lee, W. Ma, X. Gong, A.J. Heeger, Adv. Mater. **18** 572-576 (2006).
18. Effect of the Molecular Weight of Poly(3-hexylthiophene) on the Morphology and Performance of Polymer Bulk Heterojunction Solar Cells, W. Ma, J.Y. Kim, K. Lee, A.J. Heeger, Macromolecular Rapid Communications, **28**, 1776 (2007)